Geochemistry, Geophysics, Geosystems

TECHNICAL REPORTS: METHODS
10.1029/2020GC009042

A User-Friendly Workbook to Facilitate Rapid and Accurate Rare Earth Element Analyses by ICP-MS for Multispiked Samples

Y. Wu[1,2], L. D. Pena[1,3], S. L. Goldstein[1,2], C. Basak[1,4], L. L. Bolge[1], K. M. Jones[5], D. K. McDaniel[6], and S. R. Hemming[1,2]

[1]Lamont-Doherty Earth Observatory of Columbia University, Palisades, NY, USA, [2]Department of Earth and Environmental Sciences, Columbia University, Palisades, NY, USA, [3]GRC Geociències Marines, Department of Earth and Ocean Dynamics, University of Barcelona, Barcelona, Spain, [4]Department of Earth Sciences, University of Delaware, Newark, DE, USA, [5]ExxonMobil Upstream Oil and Gas: Liza Project - Phase 2, Houston, TX, USA, [6]Department of Science, Engineering and Technology, Montgomery College, Germantown, MD, USA

Abstract The rare earth elements (REEs) are widely used as geochemical tracers in the earth, planetary, and ocean sciences. Inductively coupled plasma-mass spectrometry (ICP-MS) has become the method of choice to analyze REE concentrations because it can rapidly measure the entire REE spectrum at the same time. This Technical Report presents a user-friendly "REE Calculation Workbook" in Microsoft Excel to be used for calculating REE abundances in samples equilibrated with a multielement REE spike. This Workbook can be conveniently used to calculate REE concentrations in natural samples for spiked and unspiked elements measured by ICP-MS. For the spiked elements, their concentrations are calculated using isotope dilution equations. Using these spiked elements as references, concentrations of the four mono-isotopic REE elements, and other REE elements that are treated as mono-isotopic elements (in our case, La and Lu), can be calculated. The REE Workbook can be easily set up for use with different REE spikes. Evaluation of our analytical quality using a quadrupole ICP-MS on 10-ml-sized seawater samples shows that our analyses are comparable to high-precision thermal ionization mass spectrometry (TIMS) studies, with much less time spent processing and analyzing, and with the added advantages of determining mono-isotopic elements. An important result is the clear demonstration of enrichments in Gd and Er compared to neighboring elements in seawater samples. In addition, we compare and evaluate commonly used reference standards BCR-1, Post-Archean Australian Shale (PAAS), and North American Shale Composite (NASC).

Key Points:
- A workbook deconvolves raw ICP-MS data to calculate concentrations of all the rare earth elements for multispiked samples
- Values of some common REE reference standards are evaluated
- Data quality using this approach is evaluated with seawater as an example

Supporting Information:
- Supporting Information S1
- Data Set S1

Correspondence to:
Y. Wu,
yingzhe@ldeo.columbia.edu

Citation:
Wu, Y., Pena, L. D., Goldstein, S. L., Basak, C., Bolge, L. L., Jones, K. M., et al. (2020). A user-friendly workbook to facilitate rapid and accurate rare earth element analyses by ICP-MS for multispiked samples. *Geochemistry, Geophysics, Geosystems*, *21*, e2020GC009042. https://doi.org/10.1029/2020GC009042

Received 17 MAR 2020
Accepted 29 AUG 2020
Accepted article online 4 SEPT 2020

1. Introduction

The lanthanide series, also called the rare earth elements (REEs), are a group of 15 elements from lanthanum (La, atomic number 57) to lutetium (Lu, atomic number 71), in which the electrons are progressively filled in the 4f orbitals with increasing atomic number. As a result, the REEs have similar outer electronic configurations and thus show similar chemical characteristics. The decrease of ionic radius with increasing atomic number results in small but important differences in their behavior under different geological and cosmological conditions and leads to a wide variety of applications in natural samples as geochemical tracers. For example, the "REE pattern," reflecting the degree of enrichment or depletion of light versus middle versus heavy REEs in rocks, can be used to constrain provenance or be applied to study partial melting, fractional crystallization, and magma mixing processes (e.g., Henderson, 1984). In seawater, REEs are useful tools to trace water mass mixing, redox processes, and lithogenic sources (e.g., Bertram & Elderfield, 1993; de Baar, Bacon, et al., 1985; de Baar et al., 1983; Elderfield & Greaves, 1982; German et al., 1995; Goldberg et al., 1963; Haley et al., 2014; Høgdahl et al., 1968; Lacan & Jeandel, 2001, 2004; Piper, 1974; Sholkovitz & Schneider, 1991; Zheng et al., 2016). While all the REEs are trivalent, europium (Eu) also has +2 and cerium (Ce) also has +4 charge under some natural conditions, which makes them additionally useful for evaluating redox. For example, Eu^{2+} preferentially enters plagioclase feldspar compared to neighboring REE samarium (Sm) and gadolinium (Gd), and its enrichment or depletion relative to other REEs is used to trace processes associated with plagioclase fractionation (e.g., Drake & Weill, 1975; Henderson, 1984) and even crust-mantle recycling (e.g., Sobolev et al., 2000). The enrichment or depletion of Ce compared to

Table 1
Abbreviations Used in This Paper

spk	Spike
nat	Natural
meas	Measured
abc	Acid blank correction
acid_blk	Acid blank
smpl	Sample
procedural_blk	Procedural blank
cal	Calibration
intf	Interference
oxd_cor	Oxide correction
mb	Mass bias
spkfree	Spike free
sens	Sensitivity
std	Standard
smpl_spkfree	Sample-spike free

La and praseodymium (Pr) or neodymium (Nd) is used to trace surface redox processes (e.g., Henderson, 1984; Piper, 1974). For example, Ce is highly depleted in the oxic seawater due to being scavenged in Mn oxides, which is shown as a negative Ce anomaly (e.g., German et al., 1995; Høgdahl et al., 1968; Sholkovitz & Schneider, 1991).

Total REE concentrations in natural samples range from tens of ppt (10^{-12} g/g) in seawater (global data are available in the GEOTRACES Intermediate Data Product 2017; Schlitzer et al., 2018) to hundreds of ppm (10^{-6} g/g) in samples of the Earth's crust (e.g., Taylor & McLennan, 1981; Wedepohl, 1995). The first measurements of REEs used X-ray spectrographic techniques to study REEs in meteorites (Noddack, 1935) and shales (Minami, 1935). Since the early 1960s, neutron activation analysis of REEs has been widely used for natural samples (e.g., Goldberg et al., 1963; Haskin & Haskin, 1966; Schmitt et al., 1960). Since the late 1960s, mass spectrometry has emerged as the method of choice to analyze REEs in natural samples, including thermal ionization mass spectrometry (TIMS, first reported by Schnetzler et al., 1967), secondary ion mass spectrometry (SIMS, first reported by Crozaz & Zinner, 1985), and inductively coupled plasma-mass spectrometry (ICP-MS, first reported by Jenner et al., 1990; Shabani et al., 1990). All of the mass spectrometric approaches require deconvolution of the raw data (e.g., Barbey et al., 1995, for SIMS), which go back to the beginning of using mass spectrometers (e.g., Monteiro & Reed, 1969; Washburn et al., 1943).

A common approach for calculating the concentration of an element in a sample is to add a spike (enriched in an isotope of that element) to the sample and use isotope dilution (ID) analysis (e.g., Albarède, 1996; Dickin, 1995; Heumann, 1992; Webster, 1960) to calculate the sample concentration, which is based on knowing the precise weights of the sample and spike, the isotope ratios of the natural sample and the spike, and the isotope ratio of the spike-sample mixture. The first mass spectrometric analyses of REEs in the geosciences using multi-REE spike ID date back to the late 1960s (e.g., Arth & Hanson, 1975; Gast, 1968; Schnetzler & Philpotts, 1970; Schnetzler et al., 1967). Since then the approach has been used in studies to determine REE concentrations in all kinds of natural samples (Stracke et al., 2014) including rocks (e.g., Hanson, 1980; Hooker et al., 1975; Schnetzler et al., 1967), meteorites (e.g., Evensen et al., 1978; Masuda et al., 1973; Nakamura, 1974), ferromanganese sediments (e.g., Elderfield & Greaves, 1981; Elderfield et al., 1981), seawater (e.g., Behrens et al., 2016; Bertram & Elderfield, 1993; Elderfield & Greaves, 1982; Klinkhammer et al., 1983; Pahnke et al., 2012; Piepgras & Jacobsen, 1992; Rousseau et al., 2013; Sholkovitz & Schneider, 1991; van de Flierdt et al., 2012; Zheng et al., 2015), hydrothermal fluids (e.g., Michard & Albarède, 1986; Michard et al., 1983), river water (e.g., Goldstein & Jacobsen, 1988; Sholkovitz, 1995; Sholkovitz et al., 1999), marine particles (e.g., Cullen et al., 2001; Field & Sherrell, 1998; Sholkovitz et al., 1994), and geological reference materials (e.g., Baker et al., 2002; Kent et al., 2004; Krogh Jensen et al., 2003; Raczek et al., 2001; Willbold & Jochum, 2005), among others. Using the standard ID equation (Dodson, 1963, 1969) for two isotopes, given an element x, its concentration (grams of x/grams of sample) can be calculated as

$$[x] = \frac{\left(\frac{^{i}x}{^{j}x}\right)_{\mathrm{spk}} - \left(\frac{^{i}x}{^{j}x}\right)_{\boldsymbol{meas}}}{\left(\frac{^{i}x}{^{j}x}\right)_{\boldsymbol{meas}} - \left(\frac{^{i}x}{^{j}x}\right)_{\mathrm{nat}}} \times \frac{[^{j}x]_{\mathrm{spk}}}{^{j}Ab_{\mathrm{nat}}} \times \left(\frac{m_{\mathrm{spk}}}{m_{\boldsymbol{smpl}}}\right) \times M_{x},$$

where i is a non-enriched isotope in the spike, j is the enriched isotope in the spike, $\left(^{i}x/^{j}x\right)_{\mathrm{spk}}$ is the isotope ratio in the spike, $\left(^{i}x/^{j}x\right)_{\boldsymbol{meas}}$ is the isotope ratio in the measured sample-spike mixture, $\left(^{i}x/^{j}x\right)_{\mathrm{nat}}$ is the natural isotope ratio, $[^{j}x]_{\mathrm{spk}}$ is the molar concentration of ^{j}x in the spike (mol ^{j}x/g solution), $^{j}Ab_{\mathrm{nat}}$ is the natural fractional abundance of ^{j}x (i.e., the mole fraction of ^{j}x atoms in a natural sample), m_{spk} and $m_{\boldsymbol{smpl}}$ are spike and sample weights (g), and M_x is the atomic mass of element x (g/mol). Abbreviations used in this paper are shown in Table 1.

Table 2
Analyzed Isotopes of Each Element for Samples, Procedural Blank, Pure Pr Solution, and Mass Bias Solution

Element	Analyzed isotopes			
Ba	135	137		
La	138	139		
Ce	140	142		
Pr	141			
Nd	143	144	145	146
Sm	147	148	149	
Eu	151	153		
Gd	155	157	160	
Tb	159			
Dy	161	163		
Ho	165			
Er	166	167		
Tm	169			
Yb	171	172	174	
Lu	175	176		
Hf	177			

Since ICP-MS was developed in the early 1980s (Gray & Date, 1983), it has been increasingly used for rapid multielement analysis and has become the preferred method for REE analyses. For example, REE measurements using ID-TIMS are precise but time consuming: Fractions of the REEs need to be collected, loaded onto different filaments, and analyzed separately; a sample requires ~1–3 days; and only the spiked multi-isotopic elements are measured. With ID ICP-MS analysis, many studies analyze REEs in two fractions (light and heavy REEs). In this study, by ICP-MS the entire REE spectrum of 14 elements can be analyzed in a single fraction in ~10 min. Combining the use of multielement REE spikes and ICP-MS offers a convenient means to obtain high-precision REE analyses, and because the results are based on measurement of isotope ratios, their use avoids some of the pitfalls associated with reliance on signal intensities alone.

With the increasing number of labs performing REE analyses, in order to encourage the use of multielement REE spikes, help to ensure the accuracy of the results, and promote cross laboratory consistency, this Technical Report presents an *REE Calculation Workbook* (Data Set S1 in the supporting information) for convenient use by the community to calculate REE concentrations of samples equilibrated with a multielement spike and measured by ICP-MS. The Workbook is set up for the procedure used at the Lamont-Doherty Earth Observatory (LDEO) of Columbia University, in which concentrations of eight spiked elements are determined using ID, and the concentrations of the spiked elements are used as references to calculate concentrations of the mono-isotopic REE elements, and La and Lu. The Workbook can be easily modified for other combinations of spiked and nonspiked elements.

2. Explanation of the REE Calculation Workbook

The LDEO lab uses a multielement REE spike mixed by Robert D. Vocke and calibrated by Vocke and Steven B. Shirey in Professor Gilbert Hanson's lab at Stony Brook University. The spike is enriched in ^{138}La, ^{142}Ce, ^{145}Nd, ^{149}Sm, ^{153}Eu, ^{155}Gd, ^{161}Dy, ^{167}Er, ^{171}Yb, and ^{176}Lu (Table S1). An aliquot of the stock solution was later diluted by Diane K. McDaniel (the "DKM aliquot"), who remeasured the isotope ratios and calibrated the concentrations using gravimetric REE solutions made from metal ingots. At LDEO we use a further diluted split of the Stony Brook-DKM aliquot and its calibration for the isotope ratios and the relative concentrations. We recalibrated the absolute concentrations against a Nd standard from High-Purity™ Standards Inc., with a certified ±0.3% error on the Nd concentration, using "reverse ID," where the spike is treated as the "sample" and the natural Nd standard is treated as the "spike."

This contribution uses seawater REE analyses as our example, although the Workbook can be used for any type of sample. We use seawater because it illustrates the possibility of obtaining high-quality analyses on very small samples, as discussed in section 5. LDEO methods for seawater REE analyses are described in Behrens et al. (2016). Each sample is spiked to aim for an ideal ^{145}Nd/^{143}Nd ratio for the sample-spike mixture (~9.0, Table S1) that allows for analyses of all the multi-isotope REE elements except La and Lu. After the spike is added to the acidified seawater sample, it is allowed to equilibrate for at least 24 hr. The sample-spike mixture is then purified using a commercially available preconcentration unit that separates the REEs, the sea*Fast* Automated Preconcentration System for Undiluted Seawater (Elemental Scientific Inc. or ESI, Omaha, Nebraska, USA). The sea*Fast* processing time to obtain the REE fraction is ~15 min. We analyze the samples using a VG PlasmaQuad ExCell® quadrupole ICP-MS. The instrument is coupled to a desolvating introduction system (a CETAC Aridus™) that minimizes molecular oxide ion formation with a self-aspirated Apex ST PFA micro flow nebulizer (ESI). The mass spectrometer is optimized for sensitivity and operated in pulse counting mode with 10 ms of dwell time for all isotopes. The analyzing time for a sample is ~10 min for the entire REE spectrum. The isotopes analyzed for each element are listed in Table 2.

We perform blank corrections (section 2.1), oxide corrections (section 2.2), and mass bias corrections (section 2.3) for all REEs. Then we divide the REEs into three groups and calculate their concentrations for

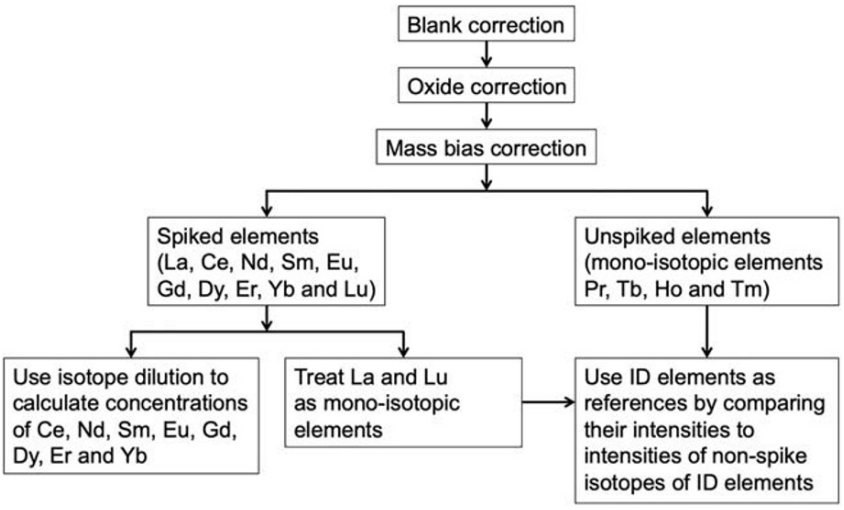

Figure 1. Flow chart summarizing the steps of REE data reduction in the REE Calculation Workbook.

ID elements (section 2.4), mono-isotopic REE elements (section 2.5), and elements treated like the mono-isotopic REE elements (section 2.6). A flow chart for the REE data reduction is summarized in Figure 1.

2.1. Blank Correction

Background intensities of REEs are measured on the mass spectrometer using a 3% nitric acid solution. All intensities for the procedural blank (this section), a pure praseodymium (Pr) solution (section 2.2), a mass bias solution (section 2.3), and samples are corrected by subtracting the counts of the 3% nitric acid blank using $I_{\mathrm{abc}} = I_{\mathrm{raw}} - I_{\boldsymbol{acid}\text{ - blk}}$, where I_{raw} is the raw intensity, $I_{\boldsymbol{acid}\text{ - blk}}$ is the intensity of the acid blank, and I_{abc} is the intensity after acid blank correction.

In our study, every batch of samples is accompanied by a procedural blank that is processed using the same method as samples. These procedural blanks provide information of how much signal comes from the whole sample processing procedure, an important step to ensure high-quality data. Sample intensities are corrected by subtracting the procedural blank using $I_{\boldsymbol{smpl}} = I_{\mathrm{abc}} - I_{\boldsymbol{procedural}\text{ - blk}}$, where I_{abc} is the intensity after acid blank correction, $I_{\boldsymbol{procedural}\text{ - blk}}$ is the intensity of the procedural blank after acid blank correction, and $I_{\boldsymbol{smpl}}$ is the intensity of sample after procedural blank correction. In our study, procedural blanks ($n = 5$) of 1% HNO_3 typically represent ≤0.9% of the sample intensities except for Ce (≤1.7%).

2.2. Oxide Correction

To correct for molecular oxide formation and interference at REE isotope masses, we perform an oxide calibration analysis by measuring masses of M and MO in pure, single element solutions of barium (Ba) and REEs. We analyze Ba and all the REEs once to construct a calibration matrix and use them, along with a measurement of Pr and PrO during each measurement session to scale up or down the oxide corrections for the individual measurement session. The isotopes analyzed for each single element solution are listed in Table 3. The oxide calibration value is expressed as the ratio of $\frac{^{MO}I_{\mathrm{cal}}}{^{M}I_{\mathrm{cal}}}$, where $^{\mathrm{M}}I_{\mathrm{cal}}$ is the intensity of mass M and $^{\mathrm{MO}}I_{\mathrm{cal}}$ is the intensity of mass MO measured during the calibration. For an unknown sample, the oxide interference for any mass M is calculated as $^{MO}I_{\boldsymbol{intf}} = \frac{^{MO}I_{\mathrm{cal}}}{^{M}I_{\mathrm{cal}}} \times {}^{M}I_{\boldsymbol{smpl}}$, where $^{\mathrm{M}}I_{\boldsymbol{smpl}}$ is the measured intensity for any mass and $^{\mathrm{MO}}I_{\boldsymbol{intf}}$ is the intensity of its oxide interference.

The oxide calibration values are not constant and can vary between different analytical sessions. Thus, oxide formation rates must be assessed and adjusted at every analytical session in which REEs are measured. However, we can assume that all the REEs show the same fractional change in oxide formation (e.g.,

Table 3
Analyzed Isotopes for Each Pure and Single Element Solutions of Ba and REE for Oxide Calibration Analysis

Analyzed elements and their oxides	Analyzed isotopes			
Ba	135	137		
BaO	151	153		
La	139			
LaO	155			
Ce	140	142		
CeO	156	158		
Pr	141			
PrO	157			
Nd	143	144	145	150
NdO	159	160	161	166
Sm	147	149	150	
SmO	163	165	166	
Eu	151	153		
EuO	167	169		
Gd	155	156	158	160
GdO	171	172	174	176
Tb	159			
TbO	175			
Dy	161			
DyO	177			

Zhao et al., 2019; http://minerva.union.edu/hollochk/icp-ms/ree_corrections.html). Therefore, we analyze the $\frac{^{157}\mathrm{PrO}}{^{141}\mathrm{Pr}}$ ratio of a 100 ng/L Pr solution during each measurement session to determine the oxide correction factor $C = \frac{\left(\frac{^{157}\mathrm{PrO}}{^{141}\mathrm{Pr}}\right)_{\boldsymbol{today}}}{\left(\frac{^{157}\mathrm{PrO}}{^{141}\mathrm{Pr}}\right)_{\mathrm{cal}}}$, where $\left(\frac{^{157}\mathrm{PrO}}{^{141}\mathrm{Pr}}\right)_{\mathrm{cal}}$ is measured during the oxide calibration analysis and $\left(\frac{^{157}\mathrm{PrO}}{^{141}\mathrm{Pr}}\right)_{\boldsymbol{today}}$ is measured each time we analyzed REEs. Then the oxide interference is expressed as $^{MO}I_{\boldsymbol{intf}} = C \times \frac{^{MO}I_{\mathrm{cal}}}{^{M}I_{\mathrm{cal}}} \times {}^{M}I_{\boldsymbol{smpl}}$. The final true intensity without oxide interference is calculated as $^{MO}I_{\mathrm{oxd\text{-}cor}} = {}^{MO}I_{\boldsymbol{smpl}} - C \times \frac{^{MO}I_{\mathrm{cal}}}{^{M}I_{\mathrm{cal}}} \times {}^{M}I_{\boldsymbol{smpl}}$.

The above calculation is based on the assumption that the ratio of $\frac{^{MO}I_{\mathrm{cal}}}{^{M}I_{\mathrm{cal}}}$ is identical in a pure, single element solution and in a sample solution. However, there is a possibility of a temperature-dependent reaction such as LaO + Ce ⇔ La + CeO in the plasma, which can add additional oxide variables in the calculating equations and result in additional uncertainties to calculate elements (e.g., Yb) with oxide interference (e.g., GdO) from an element with similar isotopic abundance (e.g., Gd) (e.g., Albalat et al., 2012). Therefore, it is very important to minimize this effect by minimizing the oxide formation in our analysis. In each REE measurement session, we adjust the gas flows to an optimal state to obtain the minimum oxide formation (0.0066 ± 0.0017, 1σ, for the Pr monitor solution) so that the oxide correction is extremely small. Our high-quality data for natural samples used for international calibration (Behrens et al., 2016; Pahnke et al., 2012; van de Flierdt et al., 2012) agree very well with results from different research groups in the world (section 5). In addition, the repeated analysis of samples yields very good long-term external reproducibility (section 5).

2.3. Mass Fractionation Correction

We use the exponential mass fractionation law $R_c = R_m \times \left(\frac{m_i}{m_j}\right)^{\beta}$ (e.g., Maréchal et al., 1999; Russell et al., 1978; Wasserburg et al., 1981) to correct for mass fractionation, where R_c is the mass fractionation corrected isotope ratio in the sample, R_m is the measured isotope ratio in the sample, m_i is the atomic mass of the spike isotope, usually the one enriched in the spike, and m_j is the atomic mass of the reference isotope. To calculate β, the exponential law mass fractionation factor, we use a mass bias solution in which each REE has concentration of 100 ng/L, and we measure it during each REE measurement session. β is expressed as $\beta = \frac{\mathrm{Ln}\left(\frac{R_n}{R_{mb}}\right)}{\mathrm{Ln}\left(\frac{m_i}{m_j}\right)}$, where R_n is the ratio in natural samples and R_{mb} is the measured ratio in the mass bias solution.

The correction for instrumental mass fractionation has very little impact on the final results of REE concentrations. The differences between mass bias corrected values and nonmass bias corrected values are within 0.1% for La, Ce, Pr, and Nd, within 1% for Tb, Ho, Er, Tm, Yb, and Lu, and within 1–2% for Sm, Gd, and Dy, and 3–4% for Eu. We use the same β values for each analytical session. Based on 59 analytical sessions, β values (1σ) are as follows: Nd, −0.9723 (±0.9942); Sm, −1.0309 (±0.7166); Eu, −1.5044 (±0.8249); Gd, 3.2681 (±5.8387); Dy, −0.8947 (±0.6918); Er, −0.1470 (±1.6342); and Yb, −0.9719 (±0.7546).

2.4. Concentrations of ID Elements

The concentrations of spiked elements are calculated using ID equations (section 1). Taking Nd as an example, we use a ^{145}Nd spike, and the Nd concentration (g Nd/g sample) is calculated as

$$[\mathrm{Nd}] = \frac{\left(\frac{^{143}\mathrm{Nd}}{^{145}\mathrm{Nd}}\right)_{\mathrm{spk}} - \left(\frac{^{143}\mathrm{Nd}}{^{145}\mathrm{Nd}}\right)_{\boldsymbol{meas}}}{\left(\frac{^{143}\mathrm{Nd}}{^{145}\mathrm{Nd}}\right)_{\boldsymbol{meas}} - \left(\frac{^{143}\mathrm{Nd}}{^{145}\mathrm{Nd}}\right)_{\mathrm{nat}}} \times \frac{\left[^{145}\mathrm{Nd}\right]_{\mathrm{spk}}}{^{145Nd}Ab_{\mathrm{nat}}} \times \frac{m_{\mathrm{spk}}}{m_{\boldsymbol{smpl}}} \times M_{\mathrm{Nd}}, \quad (1)$$

where $\left(\frac{^{143}\mathrm{Nd}}{^{145}\mathrm{Nd}}\right)_{\mathrm{spk}}$ is the isotope ratio in the spike after mass bias correction, $\left(\frac{^{143}\mathrm{Nd}}{^{145}\mathrm{Nd}}\right)_{\boldsymbol{meas}}$ is the isotope ratio in the measured sample-spike mixture after mass bias correction, $\left(\frac{^{143}\mathrm{Nd}}{^{145}\mathrm{Nd}}\right)_{\mathrm{nat}}$ is the natural isotope ratio (= 1.468), $[^{145}\mathrm{Nd}]_{\mathrm{spk}}$ is the molar concentration of ^{145}Nd in the spike (mol ^{145}Nd/g solution), $^{145\mathrm{Nd}}Ab_{\mathrm{nat}}$ is the natural abundance of ^{145}Nd (i.e., the mole fraction of ^{145}Nd atoms in a natural sample = 0.0829), m_{spk} and $m_{\boldsymbol{smpl}}$ are spike and sample weights (g), and M_{Nd} is the atomic mass of Nd (144.24 g/mol). Other elements calculated using the ID equation are Sm, Eu, Gd, Dy, Er, and Yb and henceforth will be called "ID elements."

Since ^{142}Ce has an isobaric interference from Nd, ^{142}Ce in the sample is calculated by subtracting interference of ^{142}Nd from the sample and the spike (Jones, 2010) using

$$^{142Ce}I_{\boldsymbol{smpl}} = {}^{142Total}I_{\boldsymbol{smpl}} - {}^{143Nd}I_{\boldsymbol{smpl}} \times \left(\frac{^{142}\mathrm{Nd}}{^{143}\mathrm{Nd}}\right)_{\mathrm{nat}} - {}^{143Nd}I_{\mathrm{spk}} \times \left(\frac{^{142}\mathrm{Nd}}{^{143}\mathrm{Nd}}\right)_{\mathrm{spk}},$$

where $^{142\boldsymbol{Total}}I_{\boldsymbol{smpl}}$ is the intensity of mass 142 in the sample, $^{143\mathrm{Nd}}I_{\boldsymbol{smpl}}$ is the intensity of ^{143}Nd in the sample, $\left(\frac{^{142}\mathrm{Nd}}{^{143}\mathrm{Nd}}\right)_{\mathrm{nat}}$ is the natural isotope ratio (= 2.230), $^{143\mathrm{Nd}}I_{\mathrm{spk}}$ is the intensity of ^{143}Nd in the spike (calculating equation given in Equation 2 in section 2.5), and $\left(\frac{^{142}\mathrm{Nd}}{^{143}\mathrm{Nd}}\right)_{\mathrm{spk}}$ is the isotope ratio in the spike. Then the Ce concentration is calculated using the ID Equation 1.

2.5. Concentrations of Mono-Isotopic Elements

For the mono-isotopic elements Pr, Tb, Ho, and Tm, their concentrations are calculated by comparing their intensities to intensities of nonspike isotopes of ID elements. To calculate intensities of nonspike isotopes of ID elements, contributions from the spike need to be subtracted (Jones, 2010). Taking Nd as an example, the spike-free intensity for ^{143}Nd is calculated as

$$^{143Nd}I_{\boldsymbol{spkfree}} = {}^{143Nd}I_{\boldsymbol{total}} - {}^{143Nd}I_{\mathrm{spk}} = {}^{143Nd}I_{\boldsymbol{total}} - \frac{\left(\frac{^{143}\mathrm{Nd}}{^{145}\mathrm{Nd}}\right)_{\mathrm{nat}} \times {}^{145Nd}I_{\boldsymbol{total}} - {}^{143Nd}I_{\boldsymbol{total}}}{\frac{\left(\frac{^{143}\mathrm{Nd}}{^{145}\mathrm{Nd}}\right)_{\mathrm{nat}}}{\left(\frac{^{143}\mathrm{Nd}}{^{145}\mathrm{Nd}}\right)_{\mathrm{spk}}} - 1}, \quad (2)$$

where $^{143\mathrm{Nd}}I_{\boldsymbol{total}}$ is the intensity of ^{143}Nd in total, $^{143\mathrm{Nd}}I_{\mathrm{spk}}$ is the intensity of ^{143}Nd in the spike, $^{145\mathrm{Nd}}I_{\boldsymbol{total}}$ is the intensity of ^{145}Nd in total, $\left(\frac{^{143}\mathrm{Nd}}{^{145}\mathrm{Nd}}\right)_{\mathrm{nat}}$ is the natural isotope ratio, and $\left(\frac{^{143}\mathrm{Nd}}{^{145}\mathrm{Nd}}\right)_{\mathrm{spk}}$ is the isotope ratio in the spike. Then the relationship between the intensities of the ID element and mono-isotopic element is established by comparing their sensitivities in the mass bias standard solution. Here sensitivity is defined as the ratio of the intensity of an isotope versus its concentration in a standard solution (e.g., Field & Sherrell, 1998; Kent et al., 2004; Willbold & Jochum, 2005; Willbold et al., 2003). As an example, for Nd, the sensitivity of ^{143}Nd is calculated as $^{143}\mathrm{Nd}_{\boldsymbol{sens}} = \frac{^{143Nd}I_{\mathrm{std}}}{[\mathrm{Nd}]_{\mathrm{std}} \times {}^{143Nd}Ab_{\mathrm{nat}}}$, where $^{143\mathrm{Nd}}I_{\mathrm{std}}$ is the intensity of ^{143}Nd in the standard solution, $[\mathrm{Nd}]_{\mathrm{std}}$ is the Nd concentration in the standard solution (g Nd/g solution), and $^{143\mathrm{Nd}}Ab_{\mathrm{nat}}$ is the fractional molar abundance of ^{143}Nd in a natural sample (= 0.1217). For Pr, the sensitivity of ^{141}Pr is calculated as $^{141}\mathrm{Pr}_{\boldsymbol{sens}} = \frac{^{141Pr}I_{\mathrm{std}}}{[\mathrm{Pr}]_{\mathrm{std}} \times {}^{141Pr}Ab_{\mathrm{nat}}}$, where $^{141\mathrm{Pr}}I_{\mathrm{std}}$ is the intensity of ^{141}Pr in the

standard solution, $[Pr]_{std}$ is the Pr concentration in the standard solution (g Pr/g solution), and $^{141Pr}Ab_{nat}$ is the fractional molar abundance of ^{141}Pr in a natural sample (= 1). Then the sensitivity ratio $\frac{^{143}Nd_{sens}}{^{141}Pr_{sens}}$ in the standard solution is used to calculate the Pr concentration in the sample (g Pr/g sample) using

$$[Pr]_{smpl} = \frac{^{143}Nd_{sens}}{^{141}Pr_{sens}} * \frac{^{141Pr}I_{smpl}}{^{143Nd}I_{smpl\text{-}spkfree}} \times \frac{[Nd]_{smpl} \times {}^{143Nd}Ab_{nat}}{^{141Pr}Ab_{nat}}, \quad (3)$$

where $^{141Pr}I_{smpl}$ is the intensity of ^{141}Pr in the sample, $^{143Nd}I_{smpl\text{-}spkfree}$ is the spike-free intensity for ^{143}Nd in the sample, $[Nd]_{smpl}$ is the Nd concentration in the sample (g Nd/g sample), $^{143Nd}Ab_{nat}$ is the fractional abundance of ^{143}Nd in a natural sample (= 0.1217), and $^{141Pr}Ab_{nat}$ is the fractional abundance of ^{141}Pr in a natural sample (= 1).

2.6. Concentrations of Multi-Isotope Elements Treated as Mono-Isotopic Elements

For La and Lu, ^{138}La has isobaric interferences with ^{138}Ba and ^{138}Ce and ^{176}Lu has isobaric interferences with ^{176}Yb and ^{176}Hf. In addition, ^{138}La and ^{176}Lu both have very low abundances (0.1% and 2.6%, respectively) in natural samples. Using the Stony Brook-DKM spike at LDEO, typically, only ~2% of the signal intensity on mass 138 comes from ^{138}La and ~5% of the signal intensity of mass 176 comes from ^{176}Lu. As a result, subtracting interferences adds major uncertainty to the ID calculations. For these reasons, after subtracting the ^{139}La and ^{175}Lu spike contributions, at LDEO we treat La and Lu as mono-isotopic elements, and their concentrations are calculated using equations for mono-isotopic elements.

Some multielement spikes have fewer enriched REE isotopes than the Stony Brook-DKM spike. In these cases, the Workbook can be easily modified so that they can be treated as mono-isotopic elements with their concentrations calculated using the equations for mono-isotopic elements.

3. Structure of the REE Calculation Workbook

The REE Calculation Workbook is downloadable as Data Set S1 in the supporting information. The worksheet "General Info" lists the isotopes measured during sample analysis and oxide calibration analysis. It also explains the parameters required for concentration calculations. Sample-related information is shown in blue, and spike-related information is shown in green. The worksheet "Raw Data" is used for entering the measured intensities for the blank solution, procedural blank, pure Pr solution, mass bias solution, and sample solution (in blue). The worksheet "Weights" is used for entering the sample (in blue) and spike (in green) weights for each sample. The worksheet "Spike" contains the concentrations of each isotope in the spike (in green), and the natural isotope ratios and atomic masses of these isotopes, isotopic compositions in the spike (in green) and in nature, and atomic masses of each REE element. The dilution factor (in green) is entered in the "Spike" worksheet to calculate the REE concentrations of the diluted spike. The worksheet "Isotope Abundances" contains the natural isotope abundances of Ba, each REE, and hafnium (Hf) (Holden et al., 2018). The worksheets "Blank Cor," "Oxide Cor," and "Mass Bias Cor" are used for blank correction (on 2.1), oxide correction (section 2.2), and mass bias correction (section 2.3), respectively. The worksheets "ID," "Ce," "Mono," "La," and "Lu" are used to calculate concentrations of ID elements (section 2.4), Ce (section 2.4), mono-isotopic elements (section 2.5), La (section 2.6), and Lu (section 2.6), respectively. The final results of calculated REE concentrations are shown in the worksheet "REEs."

4. Evaluation of REE Standard Reference Values for BCR-1, NASC, and PAAS

In this contribution we show as an example some REE concentrations for some seawater samples calculated using the Workbook. Information for samples and spike were entered following the instructions in section 3. Seawater REEs are usually referenced to shale standards, based on the reasoning that in seawater these elements are mainly derived from weathering of the continental surface and shales represent admixtures of large portions of the continental surface. Also, shales, like average upper continental crust, show Eu depletions when compared to solar system and planetary reference values such as bulk silicate earth or chondrites (McDonough & Sun, 1995; Rudnick & Gao, 2003), and this is propagated into seawater; normalizing seawater to shales minimizes Eu anomalies in the seawater REE patterns. An important challenge is to

Table 4
Reference Values of BCR-1, PAAS, and NASC Used in This Study and Their Sources

	BCR-1-G90	BCR-1-A94	BCR-1-J16	PAAS-TM85	PAAS-P12	NASC-G84	NASC-GJ88
La	24.9	25.0	25.46	38	44.56	31.1	34.0
Ce	53.7	53.6	53.94	80	88.25	66.7	66.7
Pr	6.80	6.90	6.765	8.9	10.15	7.90	7.93
Nd	28.8	28.6	28.68	32	37.32	27.4	30.1
Sm	6.59	6.55	6.603	5.6	6.884	5.59	5.80
Eu	1.95	1.92	1.957	1.1	1.215	1.18	1.16
Gd	6.68	6.82	6.725	4.7	6.043	5.40	5.12
Tb	1.05	1.05	1.063	0.77	0.8914	0.850	0.779
Dy	6.34	6.37	6.391	4.4	5.325	5.33	4.67
Ho	1.26	1.34	1.268	1.0	1.053	1.04	0.983
Er	3.63	3.71	3.658	2.9	3.075	3.21	2.73
Tm	0.560	0.545	0.5350	0.40	0.4510	0.500	0.414
Yb	3.38	3.39	3.377	2.8	3.012	3.06	2.67
Lu	0.510	0.497	0.4988	0.43	0.4386	0.456	0.406

Note. Concentrations are in ppm (they are also listed in pmol/kg in Table S3, often used in seawater studies). Sources: G90: Gladney et al. (1990); A94: Asmerom et al. (1994) (the multi-isotopic elements are from Goldstein & Jacobsen, 1988); J16: Jochum et al. (2016); TM85: Taylor and McLennan (1985) (the values with the exceptions of Tm and Lu are those of Nance & Taylor, 1976); P12: Pourmand et al. (2012); G84: Gromet et al. (1984); GJ88: Goldstein and Jacobsen (1988) (Lu is from Piepgras & Jacobsen, 1992; the mono-isotopic elements were measured at Harvard by quadrupole ICP-MS and are included here courtesy of S. B. Jacobsen).

decide which reference values to use. The most used shale reference standards are Post-Archean Australian Shale (PAAS), whose values are averages of analyses of multiple samples (Nance & Taylor, 1976), and the North American Shale Composite (NASC), which is a sample composed of a mixture of 40 shale samples (Haskin et al., 1966). We have evaluated these reference standards to determine which values are best to use, and the USGS Columbia River basalt reference standard BCR-1, which as a mantle partial melt should show a smooth REE pattern for all the REEs except Eu. For BCR-1 we compare three sets of reference values, the preferred values of two compilations (Gladney et al., 1990; Jochum et al., 2016) and the analyses reported in Asmerom et al. (1994), henceforth BCR-1-G90, -J16, and -A94, respectively. For PAAS we use the classic values of Taylor and McLennan (1985) and the reevaluation by Pourmand et al. (2012), henceforth PAAS-TM85 and -P12, respectively. For NASC we use Gromet et al. (1984) and Goldstein and Jacobsen (1988), henceforth NASC-G84 and -GJ88, respectively. The values used are listed in Tables 4 (in ppm) and S2 (in pmol/kg, the units often used for seawater, and ppm). The BCR-1-A94 REE values use the data from Goldstein and Jacobsen (1988) for the ID elements and Asmerom et al. (1994) added the mono-isotopic elements. The PAAS-TM85 values (Taylor & McLennan, 1985) are the same as Nance and Taylor (1976) with the exceptions of Tm and Lu. The NASC-GJ88 values include a modification to Lu (in Piepgras & Jacobsen, 1992) and until now unpublished mono-isotopic elements measured along with Lu by quadrupole ICP-MS (S. B. Jacobsen, personal communication, May 18, 2020).

We compared all seven data sets (listed in Table 4) in order to evaluate the reference values. The distilled results are shown in Figure 2; while not all of the possible data combinations are shown, those that are shown confirm our conclusions. As the differences in chemical behavior between the REEs are primarily due to the systematic changes in cationic volume, we expect that more accurate analyses would result in smoother REE patterns, excepting Ce and Eu. Comparison of the three BCR-1 values with NASC-GJ88 (which we conclude below are the best shale reference values), on a linear scale to emphasize variability (Figure 2a), shows that BCR-1-A94 is smoother than the others; therefore, we use BCR-1-A94 as our BCR-1 reference. Comparing it to the PAAS reference values (Figure 2b) shows a smoother pattern for PAAS-P12. Comparing BCR-1-A94 to the NASC reference values (Figure 2c) shows a smoother value for NASC-GJ88. These indications that NASC-GJ88 and PAAS-P12 are the better NASC and PAAS reference values are seemingly confirmed by direct comparison of the shales (Figure 2d), where normalizing NASC-GJ88 and PAAS-P12 yields a smoother REE pattern than normalizing NASC-G84 and PAAS-TM85. Finally, comparing all four shale reference values to BCR-1-A94 (Figures 2b and 2c) shows that the NASC-GJ88 has the smoothest shale REE pattern. Thus, we recommend using NASC-GJ88 (with the appropriate modifications in Table 4), PAAS-P12, and BCR-1-A94, as reference values for these standards, and NASC-GJ88 as the preferred shale reference values.

5. Evaluation of Analytical Quality From Seawater Analyses

For seawater REE studies, the LDEO lab processes ~10 ml of seawater. Concentrations have ranged between 1–9 ppt (7–64 pmol/kg) for Nd, 0.2–2 ppt (1–14 pmol/kg) for Yb, and 0.3–3 ppt (2–21 pmol/kg) for Ce (Wu, 2019). Thus for the higher abundance REEs such as Nd, the total amount of element analyzed in a sample has ranged from ~10 to 90 pg, while for the lowest abundance REEs, Tm, the amount has ranged between ~0.5 and 5 pg. For quality control, the LDEO lab repeatedly analyzes seawater samples from a GEOTRACES intercalibration station Bermuda Atlantic Time Series (BATS; 31.7°N, 64.1°W) in the North Atlantic at 20 m ($n = 18$) and 2,000 m ($n = 16$) (Figures 3a–3d and Table S3). Internal measurement errors are <2%. As expected, the long-term uncertainty is much larger than internal measurement errors and is regarded as reflecting our real uncertainty associated with measuring REEs in natural seawater. By monitoring and reporting long-term external reproducibility, we ensure that the LDEO lab is consistently producing

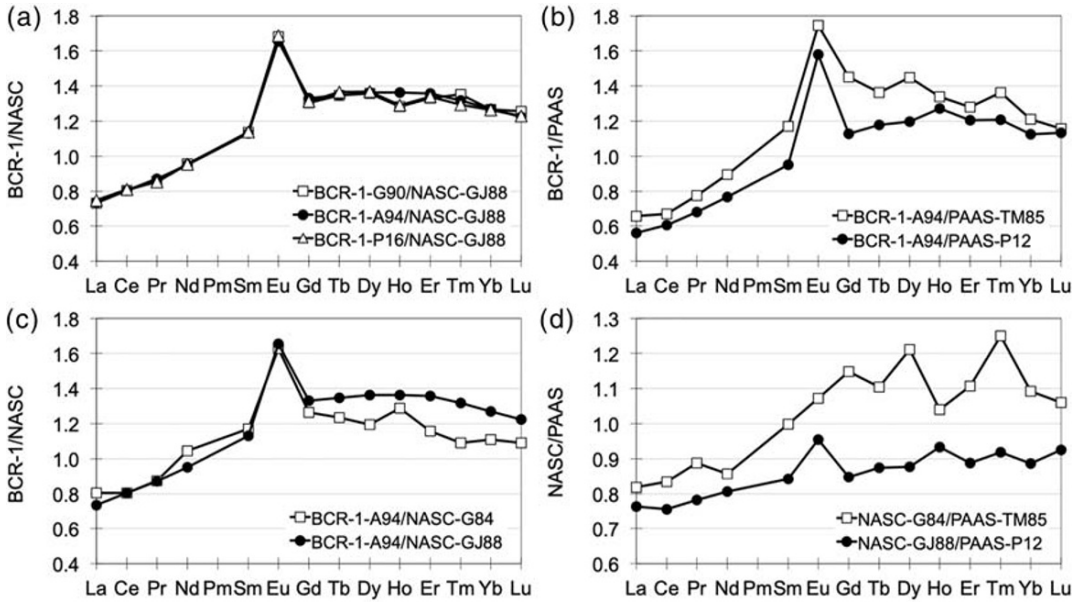

Figure 2. Comparison of published REE abundances of USGS rock standard BCR-1 (a–c), North American Shale Composite (NASC) (a, c, d), and Post-Archean Australian Shale (PAAS) (b, d). (a) Relative REE abundances of BCR-1 values from Gladney et al. (1990), Asmerom et al. (1994), and Jochum et al. (2016) normalized to NASC values from Goldstein and Jacobsen (1988). BCR-1-A94 shows the smoothest pattern. (b, c) Comparison of PAAS values from Taylor and McLennan (1985) and Pourmand et al. (2012) to BCR-1-A94. PAAS-P12 shows the smoother pattern. (c) Comparison of NASC values from Gromet et al. (1984) and Goldstein and Jacobsen (1988) to BCR-1-A94. NASC-GJ88 shows the smoother pattern. (d) Comparison of NASC and PAAS reference values, those showing smoother patterns relative to BCR-1 (NASC-GJ88 and PAAS-P12) also show smoother patterns when the four sets of reference values are compared. Thus, we recommend using BCR-1-A94, PAAS-P12, and NASC-GJ88, and between the shale normalizations, we recommend NASC-GJ88. Values and citations are listed in Table 4. For NASC-GJ88, Lu uses the updated value in Piepgras and Jacobsen (1992), and the mono-isotopic element abundances are courtesy of S. B. Jacobsen (personal communication, 2020).

high-quality data and that we realistically estimate the uncertainties that are achieved with the current technological setup.

5.1. Repeated Analyses of BATS 20 and 2,000 m Seawater

For the BATS 20 and 2,000 m samples, long-term external reproducibilities (2σ RSD%) range from 1.5% to 6.2%, depending on the element, using a two standard deviation filter on the data. Those elements showing small errors of <2% to ~5% include high (10–23 pmol/kg, for La, Ce, Nd), intermediate (3–6 pmol/kg, for Pr in the 2,000 m sample, Sm, Dy, Er, Yb), and low (0.7–0.8 pmol/kg, for Ho in the 2,000 m sample, Tb, Tm) abundance elements; this includes elements treated as mono-isotopic (La, Pr, Tb, Ho, Tm) and as ID elements (the rest). Those showing higher errors of 5–6% include both intermediate (3–5 pmol/kg for Pr in the 20 m sample, Gd) and low (Eu, Ho in the 20 m sample, Lu; 0.7–1.5 pmol/kg) abundance elements, and also elements treated as mono-isotopic (Pr, Tb, Ho, Tm) and as ID elements (the rest).

We also monitor the long-term reproducibilities of REE ratios of the BATS 20 and 2,000 m seawater samples to evaluate the quality of our analysis. The long-term external errors of La/Nd, Pr/Nd, Sm/Nd, and Yb/Nd range from 4–5% (2σ RSD) for the BATS 20 m sample and 2–5% (2σ RSD) for the BATS 2,000 m sample. The errors for REE ratios are not systematically higher or lower than the errors of the individual elements (Table S3), indicating that these are random rather than systematic errors.

5.2. BATS and SAFe Seawater Intercalibrations

The LDEO lab participated in the international intercalibration of seawater REEs from the BATS GEOTRACES station (van de Flierdt et al., 2012) that included a sample from 2,000 m. In that study, seven labs contributed, and LDEO is Lab 3 (Figures 3c and 3d and Table S3). Overall agreement for six of the seven participants (one lab's results were clear outliers) ranged from 9–12% (2σ RSD) for La, Pr, Sm, Eu, Gd, and Tb

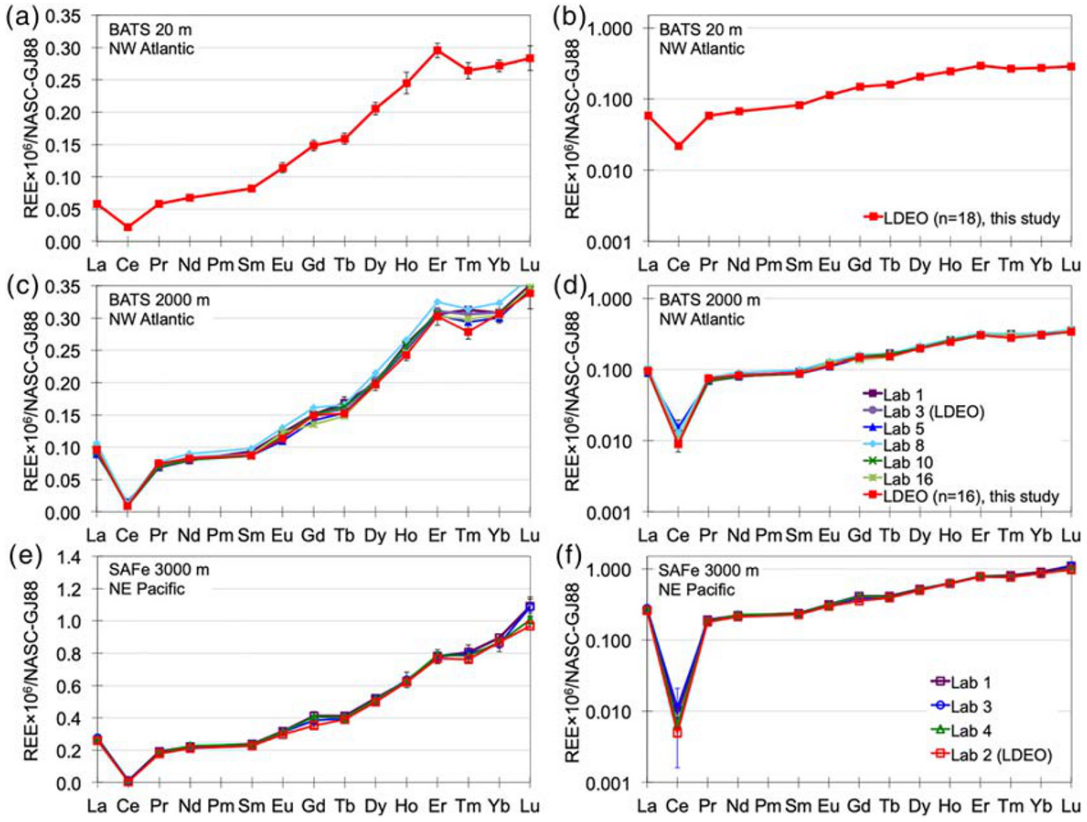

Figure 3. Average seawater REE concentrations from the BATS (Bermuda Atlantic Time Series) GEOTRACES intercalibration station (31.7°N, 64.1°W) at 20 and 2,000 m and the SAFe (Sampling and Analysis of Fe) GEOTRACES intercomparison station (30°N, 140°W) at 3,000 m, normalized to NASC-GJ88 (values from Goldstein & Jacobsen, 1988, with updates as explained in Table 4 note), on linear (a, c, e) and logarithmic (b, d, f) scales. For quality control, the LDEO lab repeatedly analyzes these BATS samples. (a, b) Average REEs for BATS 20 m sample ($n = 18$) in this study. (c, d) REEs for BATS 2,000 m ($n = 16$) in this study compared with the GEOTRACES intercalibration study (van de Flierdt et al., 2012), in which LDEO contributed data as Lab 3. (e, f) REEs for SAFe 3,000 m from the GEOTRACES intercomparison study (Behrens et al., 2016), in which LDEO contributed data as Lab 2. The error bars represent absolute two standard deviations from the mean values.

and 2–5% for all the others with the exception of Ce, where the 2σ RSD was 44%. The range of concentrations for the group showing better agreement with 2–5% 2σ RSD (0.8–17 pmol/kg) and worse agreement with 9–12% 2σ RSD (0.8–24 pmol/kg) is similar, and both groups include spiked elements and those treated as mono-isotopic elements. The higher error for Ce occurred despite a moderately high concentration of ~5 pmol/kg. A potential reason for the higher error is a higher Ce blank level compared to the other REEs (4–10%, van de Flierdt et al., 2012). Another possibility could be a sample storage artifact resulting from variable Ce oxidation in the samples of different labs. For that study LDEO contributed two analyses of the REEs from 50 to 150 ml seawater samples. Our deviations from the average values are 3–7% for La, Ce, and Eu (25, 5, and 0.9 pmol/kg, respectively) and 0–2% for all other REEs (0.7–18 pmol/kg). It is important to note that a deviation from the average does not mean that our value is less correct. In that study, our lab was the only one that used a multielement spike.

The LDEO lab also participated in a later international intercomparison of seawater REEs from GEOTRACES station Sampling and Analysis of Fe (SAFe) in the North Pacific (30°N, 140°W) at 3,000 m (Behrens et al., 2016). In that study, four labs contributed, and ours is Lab 2 (Figures 3e and 3f and Table S3). Overall agreement ranged from 2–5% 2σ RSD for all REEs (2–15 pmol/kg) except for La, Pr, Nd (6–7% 2σ RSD; 10–65 pmol/kg), Gd and Lu (12–14% 2σ RSD; 13 and 2 pmol/kg, respectively), and Ce (71% 2σ RSD; ~4 pmol/kg). Our deviations from the average values are 1–4% for all REEs except for Gd and Lu (7–9%) and Ce (38%). In that study, our lab and the University of Oldenburg used different splits of the same (Stony Brook-DKM) spike. A third lab used a spike that has ^{150}Nd, ^{172}Yb, indium, and rhenium. The fourth lab only used external standards.

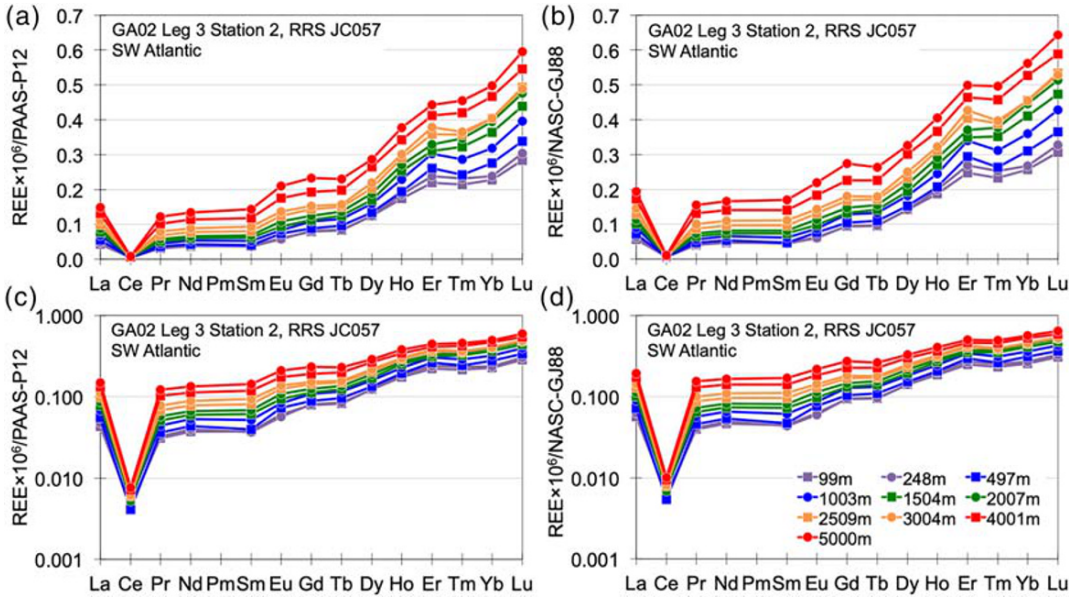

Figure 4. An example of REE results for seawater samples calculated using the REE Workbook. These seawater samples were collected between 99 and 5,000 m water depths from Station 2 (49.0°S, 48.9°W) of the GEOTRACES Southwest Atlantic Meridional Transect (RRS James Cook JC057, GA02 Leg 3) (Wu, 2019). (a–d) Relative abundances of REEs normalized to PAAS-P12 (Pourmand et al., 2012) (a, c) and NASC-GJ88 (Goldstein & Jacobsen, 1988) (b, d) on linear scales (a, b) and logarithmic scales (c, d). The depth profiles show typical seawater REE patterns, including negative Ce anomalies, HREE/LREE enrichment, and higher concentrations with increasing depth. Many of the samples clearly show positive deviations for Gd and Er.

5.3. A Seawater Station Depth Profile and Gd and Er Enrichments

The quality of the LDEO seawater results is illustrated in a depth profile (Figure 4 and Table S4) from the Southwest Atlantic (RRS James Cook JC057, GEOTRACES GA02 Leg 3, Station 2, 49.0°S, 48.9°W). The shale-normalized REE patterns are typical for seawater, with negative Ce anomalies and HREE/LREE enrichments. The absolute concentrations and the HREE/LREE enrichments both increase with increasing depth, which are also typical for seawater depth profiles. Scientific interpretations of the data are discussed in Wu (2019). We compare these results with two classic seawater REE studies that used multielement REE spikes and high-precision TIMS measurements (Bertram & Elderfield, 1993; Piepgras & Jacobsen, 1992) (Figure 5). The uncertainties reported by these studies are the internal measurement errors, better than 1% (2σ) in Piepgras and Jacobsen (1992), and better than 1% in Bertram and Elderfield (1993) except for La (2.8%), Yb (3.4%), and Lu (1.6%) (they did not report whether the uncertainty estimates were at 1σ or 2σ). Their high-precision results show smooth patterns of REE ratios such as Sm/Nd, Nd/La, and Er/La in depth profiles (Figure 5) that indicated much better data quality than previous studies that used neutron activation, where the REE ratio depth profiles show much more scattered patterns (Piepgras & Jacobsen, 1992, and Figure S1). Our results also show smooth patterns of REE ratios in depth profiles (Figure 5), indicating data quality comparable to theirs. The multielement spike ID approach thus yields high-quality data on both TIMS and quadrupole ICP-MS, with ICP-MS allowing for much faster analysis and the opportunity to analyze all the REEs at once.

A noteworthy characteristic of the Southwest Atlantic REE patterns is that they clearly show positive deviations at Gd and Er when normalized to shales (Figure 4), and although partly obscured by the Eu anomaly, they are also clearly present when normalized to BCR-1 (Figure S2). The Gd and Er positive deviations have been discussed as present in seawater REE patterns (e.g., de Baar, Brewer, et al., 1985; Kawabe et al., 1998; Masuda & Ikeuchi, 1979). Deviations of Gd and Er in particular from the otherwise smooth changes expected in REE behavior are consistent with "lanthanide tetrad effects," resulting from increased stability at 1/4 (between Nd and Pm), 1/2 (Gd), and 3/4 (between Ho and Er) filled 4f electron orbitals (e.g., Kawabe, 1992). The tetrad effect divides the REEs into four tetrad groups (first: La, Ce, Pr, Nd; second: Pm, Sm, Eu, Gd; third: Gd, Tb, Dy, Ho; fourth: Er, Tm, Yb, Lu). Because Pm is absent in nature, it is

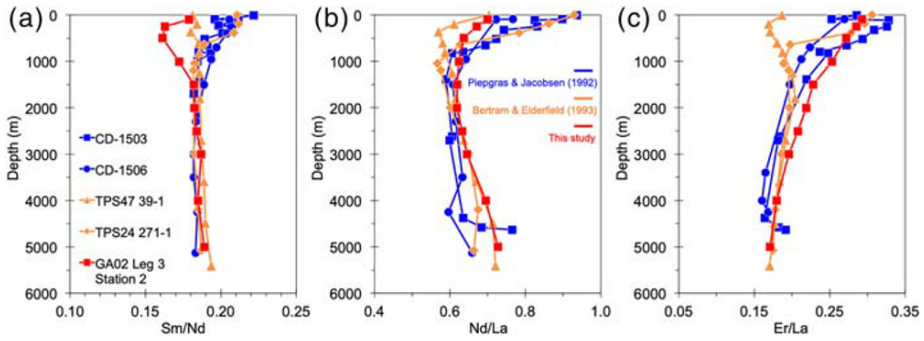

Figure 5. Depth profiles of some REE ratios for seawater samples collected from the GEOTRACES Southwest Atlantic Meridional Transect (RRS James Cook JC057, GA02 Leg 3, Station 2, 49.0°S, 48.9°W) (Table S4 and Wu, 2019) (red) measured by ICP-MS with a quadrupole mass analyzer, compared with the North Pacific seawater samples from Piepgras and Jacobsen (1992) at stations TPS47 39-1 and TPS24 271-1 (orange) and the western Indian Ocean seawater samples from Bertram and Elderfield (1993) at stations CD-1503 and CD-1506 (blue), both measured by high-precision ID-TIMS. (a) Sm/Nd depth profile. (b) Nd/La depth profile. (c) Er/La depth profile. In all three studies, these ratios vary smoothly with depth (in contrast to other approaches, Figure S1), confirming the quality of the quadrupole ICP-MS data for spiked (Sm, Nd) and unspiked (La) elements.

difficult to investigate the first tetrad effect in seawater REE patterns. The identification of both the Gd and Er positive deviations benefit from measurement of the mono-isotopic elements Tb, Ho, and Tm (Figure 4), which are not an option using TIMS but are afforded by ICP-MS analysis. While the Er anomalies are recognizable in the Piepgras and Jacobsen (1992) and Bertram and Elderfield (1993) TIMS data, with the neighboring mono-isotopic elements Ho and Tm missing, they require a four-element interpolation between Dy and Yb, making them less clear, while the ICP-MS data allow comparison with Ho and Tm. For identification of the Gd deviations, the ability to use the neighboring element mono-isotopic element Tb is critical, allowing for a three-element interpolation using Sm, as neighboring Eu cannot be used due to the possibility of a Eu anomaly.

6. Summary

This Technical Report contributes and explains an REE Calculation Workbook, in MS Excel, that reduces REE data for multielement spiked samples measured by ICP-MS, here offered for use by the community. The Report also compares and evaluates the commonly used reference standards BCR-1, PAAS, and NASC. The Workbook can be easily tailored for the needs of individual labs. It provides a convenient means for determining concentrations of all of the REEs in natural samples analyzed by ICP-MS, based on ID analysis for the spiked elements, and using ID elements as references for mono-isotopic elements and any multi-isotope elements treated as mono-isotopic elements. The data for the Stony Brook-DKM spike used at LDEO are in the REE Workbook and can be modified with concentrations and isotopic compositions of those spikes used in other labs. We show that the use of a multi-REE spike combined with ICP-MS analysis is a means to efficiently generate high-quality REE data, comparable to high-precision ID-TIMS, in about 10 min of analytical time rather than a couple of days, and including the unspiked elements. Thus, this Technical Report provides a framework to aid and encourage laboratories to adopt the multispike ID technique to measure REE concentrations by ICP-MS in natural samples.

Data Availability Statement

Data in Figures 4 and 5 and Table S4 are also available through Wu (2019).

Acknowledgments

This paper began as a short technical brief to contribute a Workbook to deconvolve the raw ICP-MS REE data, and we thank the reviewers Francis Albarède, Stein B. Jacobsen, and two other anonymous reviewers for their thorough reviews that have led to a much more comprehensive contribution. We thank reviewer S. B. Jacobsen for providing the mono-isotopic element data of NASC measured at Harvard and for suggesting that we might include it here. Interesting email discussions that included G. Hanson, M. F. Horan, J. A. Hurowitz, S. M. McLennan, E. T. Rasbury, S. B. Shirey, R. D. Vocke, and R. J. Walker illuminated the background and the calibration history of the Stony Brook multielement REE spike. We acknowledge support by NSF OCE-12-34687, NSF OCE-12-60514, and NSF OCE-14-59716 (National Science Foundation, USA), to S. L. G. and L. D. P. L. D. P. acknowledges support from Grant No. CTM2016-75411-R (MINECO, Spain). This is LDEO contribution number 8441.

References

Albalat, E., Telouk, P., & Albarède, F. (2012). Er and Yb isotope fractionation in planetary materials. *Earth and Planetary Science Letters*, *355-356*, 39–50. https://doi.org/10.1016/j.epsl.2012.08.021

Albarède, F. (1996). *Introduction to geochemical modeling*. Cambridge: Cambridge University Press.

Arth, J. G., & Hanson, G. N. (1975). Geochemistry and origin of the early Precambrian crust of northeastern Minnesota. *Geochimica et Cosmochimica Acta*, *39*(3), 325–362. https://doi.org/10.1016/0016-7037(75)90200-8

Asmerom, Y., Jacobsen, S. B., & Wernicke, B. P. (1994). Variations in magma source regions during large-scale continental extension, Death Valley region, western United States. *Earth and Planetary Science Letters*, *125*(1-4), 235–254. https://doi.org/10.1016/0012-821X(94)90218-6

Baker, J., Waight, T., & Ulfbeck, D. (2002). Rapid and highly reproducible analysis of rare earth elements by multiple collector inductively coupled plasma mass spectrometry. *Geochimica et Cosmochimica Acta*, *66*(20), 3635–3646. https://doi.org/10.1016/S0016-7037(02)00921-3

Barbey, P., Allé, P., Brouand, M., & Albarède, F. (1995). Rare-earth patterns in zircons from the Manaslu granite and Tibetan Slab migmatites (Himalaya): Insights in the origin and evolution of a crustally-derived granite magma. *Chemical Geology*, *125*(1–2), 1–17. https://doi.org/10.1016/0009-2541(95)00068-W

Behrens, M. K., Muratli, J., Pradoux, C., Wu, Y., Böning, P., Brumsack, H.-J., et al. (2016). Rapid and precise analysis of rare earth elements in small volumes of seawater—Method and intercomparison. *Marine Chemistry*, *186*, 110–120. https://doi.org/10.1016/j.marchem.2016.08.006

Bertram, C. J., & Elderfield, H. (1993). The geochemical balance of the rare earth elements and neodymium isotopes in the oceans. *Geochimica et Cosmochimica Acta*, *57*(9), 1957–1986. https://doi.org/10.1016/0016-7037(93)90087-D

Crozaz, G., & Zinner, E. (1985). Ion probe determinations of the rare earth concentrations of individual meteoritic phosphate grains. *Earth and Planetary Science Letters*, *73*(1), 41–52. https://doi.org/10.1016/0012-821X(85)90033-0

Cullen, J. T., Field, M. P., & Sherrell, R. M. (2001). Determination of trace elements in filtered suspended marine particulate material by sector field HR-ICP-MS. *Journal of Analytical Atomic Spectrometry*, *16*(11), 1307–1312. https://doi.org/10.1039/B104398F

de Baar, H. J. W., Bacon, M. P., & Brewer, P. G. (1983). Rare-earth distributions with a positive Ce anomaly in the Western North Atlantic Ocean. *Nature*, *301*(5898), 324–327. https://doi.org/10.1038/301324a0

de Baar, H. J. W., Bacon, M. P., Brewer, P. G., & Bruland, K. W. (1985). Rare earth elements in the Pacific and Atlantic Oceans. *Geochimica et Cosmochimica Acta*, *49*(9), 1943–1959. https://doi.org/10.1016/0016-7037(85)90089-4

de Baar, H. J. W., Brewer, P. G., & Bacon, M. P. (1985). Anomalies in rare earth distributions in seawater: Gd and Tb. *Geochimica et Cosmochimica Acta*, *49*(9), 1961–1969. https://doi.org/10.1016/0016-7037(85)90090-0

Dickin, A. P. (1995). *Radiogenic isotope geology*. Cambridge: Cambridge University Press.

Dodson, M. H. (1963). A theoretical study of the use of internal standards for precise isotopic analysis by the surface ionization technique: Part I—General first-order algebraic solutions. *Journal of Scientific Instruments*, *40*(6), 289–295. https://doi.org/10.1088/0950-7671/40/6/307

Dodson, M. H. (1969). A theoretical study of the use of internal standards for precise isotopic analysis by the surface ionization technique Part II: Error relationships. *Journal of Physics E: Scientific Instruments*, *2*(6), 490, 306–498. https://doi.org/10.1088/0022-3735/2/6/306

Drake, M. J., & Weill, D. F. (1975). Partition of Sr, Ba, Ca, Y, Eu^{2+}, Eu^{3+}, and other REE between plagioclase feldspar and magmatic liquid: An experimental study. *Geochimica et Cosmochimica Acta*, *39*(5), 689–712. https://doi.org/10.1016/0016-7037(75)90011-3

Elderfield, H., & Greaves, M. J. (1981). Negative cerium anomalies in the rare earth element patterns of oceanic ferromanganese nodules. *Earth and Planetary Science Letters*, *55*(1), 163–170. https://doi.org/10.1016/0012-821X(81)90095-9

Elderfield, H., & Greaves, M. J. (1982). The rare earth elements in seawater. *Nature*, *296*(5854), 214–219. https://doi.org/10.1038/296214a0

Elderfield, H., Hawkesworth, C. J., Greaves, M. J., & Calvert, S. E. (1981). Rare earth element geochemistry of oceanic ferromanganese nodules and associated sediments. *Geochimica et Cosmochimica Acta*, *45*(4), 513–528. https://doi.org/10.1016/0016-7037(81)90184-8

Evensen, N. M., Hamilton, P. J., & O'Nions, R. K. (1978). Rare-earth abundances in chondritic meteorites. *Geochimica et Cosmochimica Acta*, *42*(8), 1199–1212. https://doi.org/10.1016/0016-7037(78)90114-X

Field, M. P., & Sherrell, R. M. (1998). Magnetic sector ICPMS with desolvating micronebulization: Interference-free subpicogram determination of rare earth elements in natural samples. *Analytical Chemistry*, *70*(21), 4480–4486. https://doi.org/10.1021/ac980455v

Gast, P. W. (1968). Trace element fractionation and the origin of tholeiitic and alkaline magma types. *Geochimica et Cosmochimica Acta*, *32*(10), 1057–1086. https://doi.org/10.1016/0016-7037(68)90108-7

German, C. R., Masuzawa, T., Greaves, M. J., Elderfield, H., & Edmond, J. M. (1995). Dissolved rare earth elements in the Southern Ocean: Cerium oxidation and the influence of hydrography. *Geochimica et Cosmochimica Acta*, *59*(8), 1551–1558. https://doi.org/10.1016/0016-7037(95)00061-4

Gladney, E. S., Jones, E. A., Nickell, E. J., & Roelandts, I. (1990). 1988 compilation of elemental concentration data for USGS basalt BCR-1. *Geostandards Newsletter*, *14*(2), 209–359. https://doi.org/10.1111/j.1751-908X.1990.tb00075.x

Goldberg, E. D., Koide, M., Schmitt, R. A., & Smith, R. H. (1963). Rare-Earth distributions in the marine environment. *Journal of Geophysical Research*, *68*(14), 4209–4217. https://doi.org/10.1029/JZ068i014p04209

Goldstein, S. J., & Jacobsen, S. B. (1988). Rare earth elements in river waters. *Earth and Planetary Science Letters*, *89*(1), 35–47. https://doi.org/10.1016/0012-821X(88)90031-3

Gray, A. L., & Date, A. R. (1983). Inductively coupled plasma source mass spectrometry using continuum flow ion extraction. *Analyst*, *108*(1290), 1033–1050. https://doi.org/10.1039/AN9830801033

Gromet, L. P., Haskin, L. A., Korotev, R. L., & Dymek, R. F. (1984). The "North American shale composite": Its compilation, major and trace element characteristics. *Geochimica et Cosmochimica Acta*, *48*(12), 2469–2482. https://doi.org/10.1016/0016-7037(84)90298-9

Haley, B. A., Frank, M., Hathorne, E., & Pisias, N. (2014). Biogeochemical implications from dissolved rare earth element and Nd isotope distributions in the Gulf of Alaska. *Geochimica et Cosmochimica Acta*, *126*, 455–474. https://doi.org/10.1016/j.gca.2013.11.012

Hanson, G. N. (1980). Rare earth elements in petrogenetic studies of igneous systems. *Annual Review of Earth and Planetary Sciences*, *8*(1), 371–406. https://doi.org/10.1146/annurev.ea.08.050180.002103

Haskin, L. A., Wildeman, T. R., Frey, F. A., Collins, K. A., Keedy, C. R., & Haskin, M. A. (1966). Rare earths in sediments. *Journal of Geophysical Research (1896–1977)*, *71*(24), 6091–6105. https://doi.org/10.1029/JZ071i024p06091

Haskin, M. A., & Haskin, L. A. (1966). Rare earths in European shales: A redetermination. *Science*, *154*(3748), 507–509. https://doi.org/10.1126/science.154.3748.507

Henderson, P. (1984). *Rare earth element geochemistry*. Amsterdam: Elsevier.

Heumann, K. G. (1992). Isotope dilution mass spectrometry. *International Journal of Mass Spectrometry and Ion Processes*, *118*, 575–592. https://doi.org/10.1016/0168-1176(92)85076-C

Høgdahl, O. T., Melsom, S., & Bowen, V. T. (1968). Neutron activation analysis of lanthanide elements in sea water. In R. A. Baker (Ed.), *Trace inorganics in water* (Vol. 73, pp. 308–325). Washington, DC: ACS. https://doi.org/10.1021/ba-1968-0073.ch019

Holden, N. E., Coplen, T. B., Böhlke, J. K., Tarbox, L. V., Benefield, J., de Laeter, J. R., et al. (2018). IUPAC Periodic Table of the Elements and Isotopes (IPTEI) for the education community (IUPAC technical report). *Pure and Applied Chemistry*, *90*(12), 1833–2092. https://doi.org/10.1515/pac-2015-0703

Hooker, P. J., O'Nions, R. K., & Pankhurst, R. J. (1975). Determination of rare-earth elements in USGS standard rocks by mixed-solvent ion exchange and mass-spectrometric isotope dilution. *Chemical Geology*, *16*(3), 189–196. https://doi.org/10.1016/0009-2541(75)90027-3

Jenner, G. A., Longerich, H. P., Jackson, S. E., & Fryer, B. J. (1990). ICP-MS—A powerful tool for high-precision trace-element analysis in Earth sciences: Evidence from analysis of selected USGS reference samples. *Chemical Geology*, *83*(1–2), 133–148. https://doi.org/10.1016/0009-2541(90)90145-W

Jochum, K. P., Weis, U., Schwager, B., Stoll, B., Wilson, S. A., Haug, G. H., et al. (2016). Reference values following ISO guidelines for frequently requested rock reference materials. *Geostandards and Geoanalytical Research*, *40*(3), 333–350. https://doi.org/10.1111/j.1751-908X.2015.00392.x

Jones, K. M. (2010). *An evaluation of radiogenic isotopes as tracers of ocean circulation and sediment transport: modeling, seawater, and sediment studies* (Doctoral dissertation). New York, NY: Columbia University.

Kawabe, I. (1992). Lanthanide tetrad effect in the Ln^{3+} ionic radii and refined spin-pairing energy theory. *Geochemical Journal*, *26*(6), 309–335. https://doi.org/10.2343/geochemj.26.309

Kawabe, I., Toriumi, T., Ohta, A., & Miura, N. (1998). Monoisotopic REE abundances in seawater and the origin of seawater tetrad effect. *Geochemical Journal*, *32*(4), 213–229. https://doi.org/10.2343/geochemj.32.213

Kent, A. J. R., Jacobsen, B., Peate, D. W., Waight, T. E., & Baker, J. A. (2004). Isotope dilution MC-ICP-MS rare earth element analysis of geochemical reference materials NIST SRM 610, NIST SRM 612, NIST SRM 614, BHVO-2G, BHVO-2, BCR-2G, JB-2, WS-E, W-2, AGV-1 and AGV-2. *Geostandards and Geoanalytical Research*, *28*(3), 417–429. https://doi.org/10.1111/j.1751-908X.2004.tb00760.x

Klinkhammer, G., Elderfield, H., & Hudson, A. (1983). Rare earth elements in seawater near hydrothermal vents. *Nature*, *305*(5931), 185–188. https://doi.org/10.1038/305185a0

Krogh Jensen, K., Baker, J., Waight, T., Frei, R., & Peate, D. W. (2003). High precision Ru, Pd, Ir, Pt, Re and REE determinations in the Stevns Klint Cretaceous-Tertiary Boundary reference material (FC-1) by isotope dilution multiple collector inductively coupled plasma-mass spectrometry. *Geostandards Newsletter*, *27*(1), 59–66. https://doi.org/10.1111/j.1751-908X.2003.tb00712.x

Lacan, F., & Jeandel, C. (2001). Tracing Papua New Guinea imprint on the central Equatorial Pacific Ocean using neodymium isotopic compositions and Rare Earth Element patterns. *Earth and Planetary Science Letters*, *186*(3–4), 497–512. https://doi.org/10.1016/S0012-821X(01)00263-1

Lacan, F., & Jeandel, C. (2004). Neodymium isotopic composition and rare earth element concentrations in the deep and intermediate Nordic Seas: Constraints on the Iceland Scotland Overflow Water signature. *Geochemistry, Geophysics, Geosystems*, *5*, n/a. https://doi.org/10.1029/2004GC000742

Maréchal, C. N., Télouk, P., & Albarède, F. (1999). Precise analysis of copper and zinc isotopic compositions by plasma-source mass spectrometry. *Chemical Geology*, *156*(1–4), 251–273. https://doi.org/10.1016/S0009-2541(98)00191-0

Masuda, A., & Ikeuchi, Y. (1979). Lanthanide tetrad effect observed in marine environment. *Geochemical Journal*, *13*(1), 19–22. https://doi.org/10.2343/geochemj.13.19

Masuda, A., Nakamura, N., & Tanaka, T. (1973). Fine structures of mutually normalized rare-earth patterns of chondrites. *Geochimica et Cosmochimica Acta*, *37*(2), 239–248. https://doi.org/10.1016/0016-7037(73)90131-2

McDonough, W. F., & Sun, S. s. (1995). The composition of the Earth. *Chemical Geology*, *120*(3-4), 223–253. https://doi.org/10.1016/0009-2541(94)00140-4

Michard, A., & Albarède, F. (1986). The REE content of some hydrothermal fluids. *Chemical Geology*, *55*(1–2), 51–60. https://doi.org/10.1016/0009-2541(86)90127-0

Michard, A., Albarede, F., Michard, G., Minster, J. F., & Charlou, J. L. (1983). Rare-earth elements and uranium in high-temperature solutions from East Pacific Rise hydrothermal vent field (13 °N). *Nature*, *303*(5920), 795–797. https://doi.org/10.1038/303795a0

Minami, E. (1935). Gehalte seltener Erden in europäischen und japanischen Tonschiefern. *Nachrichten von der Gesellschaft der Wissenschaften zu Göttingen, Math-Physik Klasse IV*, *1*(1), 155–170.

Monteiro, L. F., & Reed, R. I. (1969). Mass spectra and molecular structure. Part II. The analysis of mixtures. *International Journal of Mass Spectrometry and Ion Physics*, *2*(3), 265–285. https://doi.org/10.1016/0020-7381(69)80023-9

Nakamura, N. (1974). Determination of REE, Ba, Fe, Mg, Na and K in carbonaceous and ordinary chondrites. *Geochimica et Cosmochimica Acta*, *38*(5), 757–775. https://doi.org/10.1016/0016-7037(74)90149-5

Nance, W. B., & Taylor, S. R. (1976). Rare earth element patterns and crustal evolution—I. Australian post-Archean sedimentary rocks. *Geochimica et Cosmochimica Acta*, *40*(12), 1539–1551. https://doi.org/10.1016/0016-7037(76)90093-4

Noddack, I. (1935). Die Häufigkeiten der seltenen Erden in Meteoriten. *Zeitschrift für Anorganische und Allgemeine Chemie*, *225*(4), 337–364. https://doi.org/10.1002/zaac.19352250408

Pahnke, K., Van de Flierdt, T., Jones, K. M., Lambelet, M., Hemming, S. R., & Goldstein, S. L. (2012). GEOTRACES intercalibration of neodymium isotopes and rare earth element concentrations in seawater and suspended particles. Part 2: Systematic tests and baseline profiles. *Limnology and Oceanography: Methods*, *10*(4), 252–269. https://doi.org/10.4319/lom.2012.10.252

Piepgras, D. J., & Jacobsen, S. B. (1992). The behavior of rare earth elements in seawater: Precise determination of variations in the North Pacific water column. *Geochimica et Cosmochimica Acta*, *56*(5), 1851–1862. https://doi.org/10.1016/0016-7037(92)90315-A

Piper, D. Z. (1974). Rare earth elements in the sedimentary cycle: A summary. *Chemical Geology*, *14*(4), 285–304. https://doi.org/10.1016/0009-2541(74)90066-7

Pourmand, A., Dauphas, N., & Ireland, T. J. (2012). A novel extraction chromatography and MC-ICP-MS technique for rapid analysis of REE, Sc and Y: Revising CI-chondrite and Post-Archean Australian Shale (PAAS) abundances. *Chemical Geology*, *291*, 38–54. https://doi.org/10.1016/j.chemgeo.2011.08.011

Raczek, I., Stoll, B., Hofmann, A. W., & Peter Jochum, K. (2001). High-precision trace element data for the USGS reference materials BCR-1, BCR-2, BHVO-1, BHVO-2, AGV-1, AGV-2, DTS-1, DTS-2, GSP-1 and GSP-2 by ID-TIMS and MIC-SSMS. *Geostandards Newsletter*, *25*(1), 77–86. https://doi.org/10.1111/j.1751-908X.2001.tb00789.x

Rousseau, T., Sonke, J. E., Chmeleff, J., Candaudap, F., Lacan, F., Boaventura, G., et al. (2013). Rare earth element analysis in natural waters by multiple isotope dilution–sector field ICP-MS. *Journal of Analytical Atomic Spectrometry*, *28*(4), 573–584. https://doi.org/10.1039/C3JA30332B

Rudnick, R. L., & Gao, S. (2003). Composition of the continental crust. In R. L. Rudnick (Ed.), *The crust* (Vol. 3, pp. 1–64). New York: Elsevier Science.

Russell, W. A., Papanastassiou, D. A., & Tombrello, T. A. (1978). Ca isotope fractionation on the Earth and other solar system materials. *Geochimica et Cosmochimica Acta*, *42*(8), 1075–1090. https://doi.org/10.1016/0016-7037(78)90105-9

Schlitzer, R., Anderson, R. F., Dodas, E. M., Lohan, M., Geibert, W., Tagliabue, A., et al. (2018). The GEOTRACES Intermediate Data Product 2017. *Chemical Geology*, *493*, 210–223. https://doi.org/10.1016/j.chemgeo.2018.05.040

Schmitt, R. A., Mosen, A. W., Suffredini, C. S., Lasch, J. E., Sharp, R. A., & Olehy, D. A. (1960). Abundances of the rare-earth elements, lanthanum to lutetium, in chondritic meteorites. *Nature*, *186*(4728), 863–866. https://doi.org/10.1038/186863a0

Schnetzler, C. C., & Philpotts, J. A. (1970). Partition coefficients of rare-earth elements between igneous matrix material and rock-forming mineral phenocrysts—II. *Geochimica et Cosmochimica Acta*, *34*(3), 331–340. https://doi.org/10.1016/0016-7037(70)90110-9

Schnetzler, C. C., Thomas, H. H., & Philpotts, J. A. (1967). Determination of rare earth elements in rocks and minerals by mass spectrometric, stable isotope dilution technique. *Analytical Chemistry*, *39*(14), 1888–1890. https://doi.org/10.1021/ac50157a073

Shabani, M. B., Akagi, T., Shimizu, H., & Masuda, A. (1990). Determination of trace lanthanides and yttrium in seawater by inductively coupled plasma mass spectrometry after preconcentration with solvent extraction and back-extraction. *Analytical Chemistry*, *62*(24), 2709–2714. https://doi.org/10.1021/ac00223a012

Sholkovitz, E. R. (1995). The aquatic chemistry of rare earth elements in rivers and estuaries. *Aquatic Geochemistry*, *1*(1), 1–34. https://doi.org/10.1007/BF01025229

Sholkovitz, E. R., Elderfield, H., Szymczak, R., & Casey, K. (1999). Island weathering: River sources of rare earth elements to the Western Pacific Ocean. *Marine Chemistry*, *68*(1–2), 39–57. https://doi.org/10.1016/S0304-4203(99)00064-X

Sholkovitz, E. R., Landing, W. M., & Lewis, B. L. (1994). Ocean particle chemistry: The fractionation of rare earth elements between suspended particles and seawater. *Geochimica et Cosmochimica Acta*, *58*(6), 1567–1579. https://doi.org/10.1016/0016-7037(94)90559-2

Sholkovitz, E. R., & Schneider, D. L. (1991). Cerium redox cycles and rare earth elements in the Sargasso Sea. *Geochimica et Cosmochimica Acta*, *55*(10), 2737–2743. https://doi.org/10.1016/0016-7037(91)90440-G

Sobolev, A. V., Hofmann, A. W., & Nikogosian, I. K. (2000). Recycled oceanic crust observed in 'ghost plagioclase' within the source of Mauna Loa lavas. *Nature*, *404*(6781), 986–990. https://doi.org/10.1038/35010098

Stracke, A., Scherer, E. E., & Reynolds, B. C. (2014). 15.4—Application of isotope dilution in geochemistry. In H. D. Holland, & K. K. Turekian (Eds.), *Treatise on geochemistry* (Second ed.pp. 71–86). Oxford: Elsevier. https://doi.org/10.1016/B978-0-08-095975-7.01404-2

Taylor, S. R., & McLennan, S. M. (1981). The composition and evolution of the continental crust: Rare earth element evidence from sedimentary rocks. *Philosophical Transactions of the Royal Society of London. Series A, Mathematical and Physical Sciences*, *301*(1461), 381–399. https://doi.org/10.1098/rsta.1981.0119

Taylor, S. R., & McLennan, S. M. (1985). *The continental crust: Its composition and evolution*. Oxford: Blackwell Scientific.

van de Flierdt, T., Pahnke, K., Amakawa, H., Andersson, P., Basak, C., Coles, B., et al. (2012). GEOTRACES intercalibration of neodymium isotopes and rare earth element concentrations in seawater and suspended particles. Part 1: Reproducibility of results for the international intercomparison. *Limnology and Oceanography: Methods*, *10*(4), 234–251. https://doi.org/10.4319/lom.2012.10.234

Washburn, H., Wiley, H., & Rock, S. (1943). The mass spectrometer as an analytical tool. *Industrial and Engineering Chemistry, Analytical Edition*, *15*(9), 541–547. https://doi.org/10.1021/i560121a001

Wasserburg, G. J., Jacobsen, S. B., DePaolo, D. J., McCulloch, M. T., & Wen, T. (1981). Precise determination of Sm/Nd ratios, Sm and Nd isotopic abundances in standard solutions. *Geochimica et Cosmochimica Acta*, *45*(12), 2311–2323. https://doi.org/10.1016/0016-7037(81)90085-5

Webster, R. K. (1960). Mass spectrometric isotope dilution analysis. In A. A. Smales, & L. R. Wager (Eds.), *Methods in geochemistry* (pp. 202–246). New York: Interscience.

Wedepohl, K. H. (1995). The composition of the continental crust. *Geochimica et Cosmochimica Acta*, *59*(7), 1217–1232. https://doi.org/10.1016/0016-7037(95)00038-2

Willbold, M., & Jochum, K. P. (2005). Multi-element isotope dilution sector field ICP-MS: A precise technique for the analysis of geological materials and its application to geological reference materials. *Geostandards and Geoanalytical Research*, *29*(1), 63–82. https://doi.org/10.1111/j.1751-908X.2005.tb00656.x

Willbold, M., Jochum, K. P., Raczek, I., Amini, M. A., Stoll, B., & Hofmann, A. W. (2003). Validation of multi-element isotope dilution ICPMS for the analysis of basalts. *Analytical and Bioanalytical Chemistry*, *377*(1), 117–125. https://doi.org/10.1007/s00216-003-2037-4

Wu, Y. (2019). *Investigating the applications of neodymium isotopic compositions and rare earth elements as water mass tracers in the South Atlantic and North Pacific* (Doctoral dissertation). New York, NY: Columbia University. https://doi.org/10.7916/d8-kstx-xg38

Zhao, W., Zong, K., Liu, Y., Hu, Z., Chen, H., & Li, M. (2019). An effective oxide interference correction on Sc and REE for routine analyses of geological samples by inductively coupled plasma-mass spectrometry. *Journal of Earth Science*, *30*(6), 1302–1310. https://doi.org/10.1007/s12583-019-0898-5

Zheng, X. Y., Plancherel, Y., Saito, M. A., Scott, P. M., & Henderson, G. M. (2016). Rare earth elements (REEs) in the tropical South Atlantic and quantitative deconvolution of their non-conservative behavior. *Geochimica et Cosmochimica Acta*, *177*, 217–237. https://doi.org/10.1016/j.gca.2016.01.018

Zheng, X. Y., Yang, J., & Henderson, G. M. (2015). A robust procedure for high-precision determination of rare earth element concentrations in seawater. *Geostandards and Geoanalytical Research*, *39*(3), 277–292. https://doi.org/10.1111/j.1751-908X.2014.00307.x